$$2n_1k_1 = \frac{\epsilon_1}{\epsilon_0\omega} \frac{\omega_p^2\tau}{[1 + \tau^2(\omega \pm \omega_c)^2]},$$

where ϵ_1 is the lattice dielectric constant, $\omega_p = ne^2/\epsilon_1 m^*$, ω the incident photon frequency, and τ the electron scattering time.

The procedure of computer fitting is to alternatively adjust the two unknown parameters τ and m^* in ω_p and ω_c to minimize the deviation at each point. The crosses in Fig. 3 are the calculated values from best fit (with standard deviation 2%) to the experimental data. The fitting parameters are $m^* = 0.063m_0$ and $\tau = 2.72 \times 10^{-13}$ s, corresponding to $\mu = 7700$ cm^2/Vs. We would like to point out that the electron effective mass is $0.068m_0$ in GaAs and $0.048m_0$ in GaSb. By using linear extrapolation, the electron effective mass is $\sim 0.062m_0$ in $GaAs_{0.7}Sb_{0.3}$, which agrees quite well with our result.

In conclusion, we have investigated the transport properties of a GaAsSb-AlGaAs SLS, using low field Hall measurements from 4.2 to 300 K, high field quantum transport, and the far-infrared cyclotron resonance at 4.2 K. The existence of a 2DEG with an electron mobility of 7700 cm^2/Vs in our sample suggests that high quality semiconductor superlattices with controllable electrical and optical characteristics are possible in the GaAsSb-AlGaAs modulation-doped heterostructure using the SLS scheme.

The work at Princeton University is supported by the Office of Naval Research through contract No. N00014-82-K-0450 and the work at the University of Illinois by the Air Force Office of Scientific Research.

[1]L. Esaki and R. Tsu, IBM J. Res. Develop. **14**, 61 (1970).
[2]F. C. Frank and J. H. van der Merwe, Proc. R. Soc. London A **198**, 216 (1949).
[3]J. H. van der Merwe, J. Appl. Phys. **34**, 117 (1963).
[4]J. W. Matthews and A. E. Blakeslee, J. Cryst. Growth **27**, 118 (1974); **29**, 273 (1975).
[5]T. E. Zipperian, L. R. Dawson, G. C. Osbourn, and I. J. Fritz, International Electron Devices Meeting, Washington D.C., **IEDM-83**, 696 (1983).
[6]G. C. Osbourn, I. J. Fritz, R. M. Biefeld, P. L. Gourley, J. J. Wiczer, and R. J. Chaffin, IEEE Tran. Electron Devices **ED-29**, 1689 (1982).
[7]J. P. Noblanc, Appl. Phys. **13**, 211 (1977).
[8]C. C. Chang, R. Ludeke, L. L. Chang, and L. Esaki, Appl. Phys. Lett. **31**, 759 (1977).
[9]H. L. Stormer, R. Dingle, A. C. Gossard, W. Wiegmann, and M. D. Sturge, Solid State Commun. **29**, 705 (1979).
[10]B. J. F. Lin. D. C. Tsui, M. Paalanen, and A. C. Gossard, Appl. Phys. Lett. **45**, 695 (1984).
[11]D. C. Tsui and A. C. Gossard, Appl. Phys. Lett. **38**, 550 (1981).
[12]R. L. Petritz, Phys. Rev. **110**, 1254 (1958).
[13]R. J. Elliot and A. F. Gibson, *An Introduction to Solid State Physics and its Applications* (Macmillan, London, 1978), p. 274.

Hot-electron memory effect in double-layered heterostructures

S. Luryi
AT&T Bell Laboratories, Murray Hill, New Jersey 07974

A. Kastalsky
Bell Communications Research, Incorporated, Murray Hill, New Jersey 07974

A. C. Gossard and R. Hendel
AT&T Bell Laboratories, Murray Hill, New Jersey 07974

(Received 4 September 1984; accepted for publication 26 September 1984)

We studied a memory effect due to the real-space hot-electron transfer between two conducting GaAs layers separated by a graded AlGaAs barrier. Application of a lateral electric field to one of the layers enhances its electron temperature and leads to a charge injection into the other layer which is kept floating. As the heating voltage is removed, the injected electrons remain in the second layer, giving rise (at low temperatures, 77 K) to a persistent potential difference. Kinetics of the charge-up process are studied at different heating voltages.

The effect of real-space hot-electron transfer in multilayer semiconductor structures was first suggested by Hess *et al.*[1] Recently we proposed[2] a novel structure in which this phenomenon gives rise to a charge injection between two conducting layers isolated by a potential barrier and contacted separately. Several new high-speed semiconductor devices based on this mechanism have been proposed[2] and experimentally demonstrated.[3,4] In the present paper we describe a memory effect observed in our charge-injection structure.

The device is implemented in a AlGaAs/GaAs heterostructure, as shown schematically in Fig. 1. Details of its growth and processing can be found in Ref. 4. One of the conducting layers is realized as a (selectively doped heterojunction) field-effect transistor (FET) channel, the other as a heavily doped GaAs substrate. The layers are separated by an AlGaAs graded barrier. Application of a source-to-drain voltage V_{SD} leads to a heating of channel electrons and charge injection into the substrate. There is a fourth (gate) terminal whose purpose is to control the electric field distri-

 © 1984 American Institute of Physics

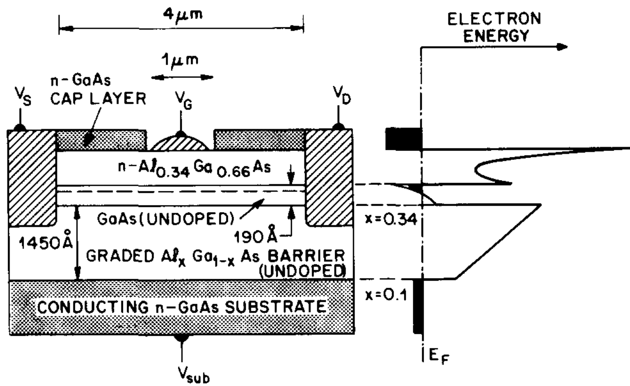

FIG. 1. Experimental structure and its energy diagram.

bution in the channel, concentrating it in a narrow (1 μm) region under the gate notch. If a positive bias is applied to the substrate, then the hot-electron injection from the channel results in a steady-state current $I_{sub,}$ controlled by the heating voltage V_{SD} This process is accompanied by a pronounced negative differential resistance in the drain circuit. These effects underlie the operation of high-speed devices studied in Refs. 3 and 4.

In the present work we study the situation in which the substrate is floating. In this case the hot-electron injection charges up the substrate thus depleting the channel. The resultant rise in the substrate potential (thermoelectric force of hot electrons) is applied to the substrate-to-channel triangular-barrier diode in the forward direction. A steady-state situation obtains when the "cold" thermionic emission exactly balances the hot-electron injection.[2] If one now removes the heating voltage, one can expect a retention of charge in the substrate for a period of time controlled by the cold thermionic emission. In this case the substrate acts as a "giant trap" for injected electrons.[5]

Experimental demonstration of this effect at 77 K is presented in Fig. 2. The solid line shows the development of the substrate potential ψ_{sub} (relative to the grounded drain) as a function of V_{SD}. This potential is measured with a high-impedance ($10^{14}\ \Omega$) electrometer. As the heating voltage is slowly increased, we reach a point $V_{SD} \approx 0.3$ V at which ψ_{sub} rises sharply and saturates at $\psi_{sub} \approx 0.2$ V within several seconds. At the same time the drain current drops by about 30%, as indicated by the broken line in Fig. 2. Since this drop occurs well below the FET saturation regime, we can estimate the amount of transferred charge $\Delta\sigma$ by assuming that prior to the transfer the channel has an equilibrium electron concentration σ_0. From the measured $\sigma_0 = 5\times 10^{11}$ cm^{-2} we have $\Delta\sigma \approx 1.5\times 10^{11}$ cm^{-2}. This amount of charge transferred to the distance 1450 Å (the barrier thickness) correlates with the measured potential $\psi_{sub} \approx 0.2$ V. Further increase of the heating voltage above $V_{SD} = 0.3$ V leads to a smooth rise of ψ_{sub}. In this region the dependence ψ_{sub} (V_{SD}) is not hysteretic. On the other hand, as we decrease V_{SD} below 0.3 V we see a strong hysteresis in both ψ_{sub} and I_{SD}. The residual potential $\psi_{sub}(0) = 0.18$ V holds for the long time controlled by a discharge through the electrometer. If the latter is disconnected, the residual potential does not change measurably for several hours.

As mentioned above, at $V_{SD} = 0.3$ V the rise time of

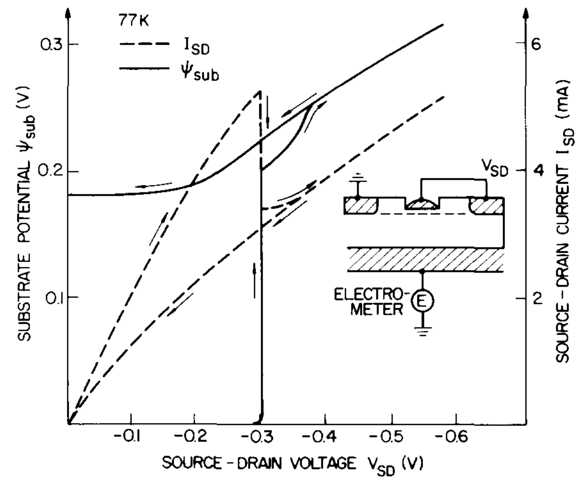

FIG. 2. Substrate potential ψ_{sub} and the channel current I_{SD} as functions of the heating voltage V_{SD}. Arrows indicate the direction of slow (10 mV/s) voltage ramping.

ψ_{sub} is of order several seconds. However, at higher heating voltages the charge-up rate is dramatically enhanced. We investigated the charge-up kinetics by applying the heating voltage V_{SD} in the form of a single rectangular pulse of variable amplitude and duration, Fig. 3. For the pulse duration $\Delta t = 10^{-4}$ s the dependence $\psi_{sub}(V_{SD})$ exhibits a sharp rise starting from the pulse amplitude $V_{SD} \approx 0.4$ V. After each measurement the device was returned to its equilibrium state by grounding the substrate. For $V_{SD} \gtrsim 0.6$ V the resultant charge-up reaches its maximum value 0.18 V, equal to the residual ψ_{sub} in Fig. 2. This means that for $V_{SD} = 0.6$ V it takes about 100μs to complete the charge transfer. At higher pulse amplitudes this time is considerably shorter. The dependence of the pulse time Δt necessary to complete the

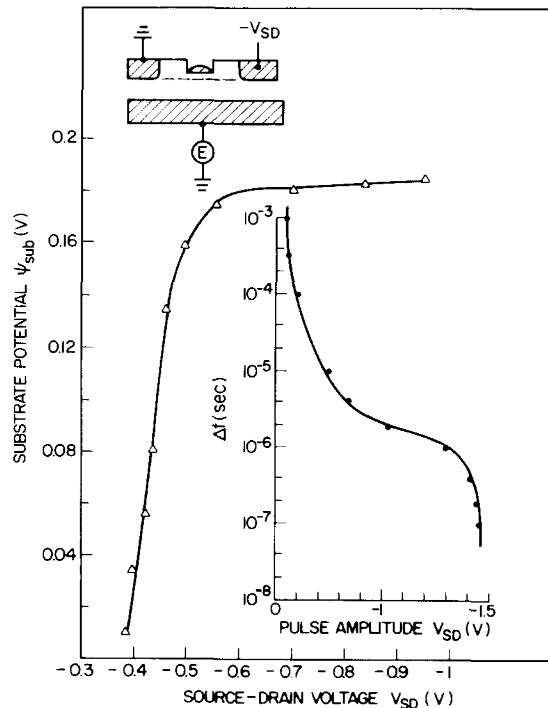

FIG. 3. Residual substrate potential ψ_{sub} after a single pulse ($\Delta t = 100\mu$s) of the heating voltage of amplitude V_{SD}. Insert shows the pulse duration Δt which provides the maximum residual potential $\psi_{sub} = 0.18$ V at a given pulse amplitude V_{SD}.

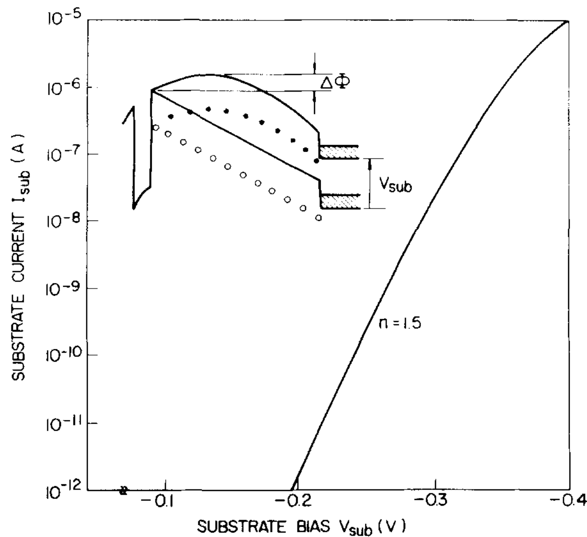

FIG. 4 Forward-bias current-voltage characteristic of the substrate-to-channel triangular-barrier diode. Insert illustrates the distortion of the barrier shape due to electron trapping. Circles indicate the trap level. Filled circles correspond to occupied traps.

transfer (i.e., to reach the maximum persistent $\psi_{sub} = 0.18$ V) on the pulse amplitude V_{SD} is shown in the insert in Fig. 3. We see a rapid decrease of Δt when $V_{SD} \gtrsim 1.3$ V. It should be noted that these time dependence measurements are not directly related to the intrinsic time of the memory charge-up, since the hot-electron current must also charge all the parasitic capacitances between the substrate and the ground (~ 100 pF). The intrinsic device capacitance (substrate to channel) can be estimated to be ~ 1 pF, which means that according to our data in Fig. 3 the ideal memory charge-up time should be less than 10^{-9} s at the pulse amplitude of order 1.5 V.

We now return to the data in Fig. 2. It is physically clear why the curves are nonhysteretic at $V_{SD} \gtrsim 0.4$ V: at high heating levels the steady-state balance between the hot and the cold electron currents is established at much higher fluxes in each direction. On the other hand, there is a small hysteresis at $V_{SD} \approx 0.3$ V, which, in our view, is associated with electron trapping in the barrier region. We have independent evidence for the existence of traps in the nominally undoped AlGaAs barrier at the level of $\sim 10^{16}$ cm^{-3}.

This evidence comes from the analysis of the forward-bias IV characteristic of the substrate-to-channel diode, Fig. 4. For an ideal triangular-barrier of the form shown in Fig. 1 one would expect an ideality factor $n \sim 1$ (neglecting the channel thickness). However, the curve in Fig. 4 corresponds to $n = 1.5$ at low currents. This curve was measured in the dark and after prebiasing the diode at 0.5 V in the forward direction. Under these conditions the curve is stable and nonhysteretic. We believe that after the initial forward biasing the barrier traps are fully charged changing the shape of the barrier as shown in the insert to Fig. 4. The experimental curve can be fitted by assuming a uniform density of electrons trapped on the barrier equal to 1.5×10^{16} cm^{-3}. This concentration of traps in the undoped AlGaAs region is consistent with recent results of other workers.[6] Finally, the curve in Fig. 4 allows us to estimate the barrier height Φ for thermionic emission under trap-filled conditions. We find $\Phi = 0.32$ eV which is somewhat higher that what one would expect for a GaAs/$Al_{0.34}Ga_{0.66}As$ heterojunction (assuming the recently proposed[7] conduction-band discontinuity rule $\Delta E_c \approx 0.6 \Delta E_{gap}$ the expected $\Phi = 0.25$ eV). The difference $\Delta\Phi \approx 0.07$ eV can thus be attributed to the space-charge potential of trapped electrons.

The authors wish to thank W. Wiegmann for the growth of structures.

[1]K. Hess, H. Morkoç, H. Shichijo, and B. G. Streetman, Appl. Phys. Lett. **35**, 469 (1979); see also K. Hess, Physica B **117**, 723 (1983) and references therein.
[2]A. Kastalsky and S. Luryi, IEEE Electron Device Lett. **EDL-4**, 334 (1983).
[3]A. Kastalsky, S. Luryi, A. C. Gossard, and R. Hendel, IEEE Electron Device Lett. **EDL-5**, 57 (1984).
[4]S. Luryi, A. Kastalsky, A. C. Gossard, and R. Hendel, IEEE Trans. Electron Devices **ED-31**, 832 (1984).
[5]P. J. Price, IEEE Trans. Electron Devices **ED-28**, 911 (1981).
[6]T. Hickmott (private communication).
[7]R. C. Miller, D. A. Kleinman, and A. C. Gossard, Phys. Rev. B **29**, 7085 (1984); W. I. Wang, E. E. Mendez, and F. Stern, Appl. Phys. Lett. **45**, 639 (1984).